Lab report
E213 Analysis of Z^0 Decay

Chenhuan Wang and Harilal Bhattarai

October 15, 2020

This is abstract.

1. Introduction

This is introduction.

2. Theory

Decay width The partial decay width of Z^0 decay into fermion f is

$$\Gamma_f = \frac{\sqrt{2}N_c^f}{12\pi} G_F M_Z^3 \left((g_V^f)^2 + (g_A^f)^2 \right) \tag{1}$$

with

$$g_V^f = I_3^f - 2Q_f \sin^2\theta_W$$
$$g_A^f = I_3^f$$

One needs to be aware that Γ_f contains contribution from both chiralities, and I_3 here refers to only the weak isospin of left-handed fermions (by definition right handed fermions have no weak isospin).

Partial cross section of $Z^0 \to f\bar{f}$ is given by [1]

$$\sigma_f(s) = \frac{12\pi}{M_Z^2} \frac{s\Gamma_e\Gamma_f}{(s-M_Z^2)^2 + (s^2\Gamma_Z^2/M_Z^2)} \tag{2}$$

Angular distribution In $ee \to ee$ scattering, two relevant channels have different angular dependences. For s-channel,

$$\frac{\mathrm{d}\sigma}{\mathrm{d}\Omega}_s \sim (1+\cos^2\Theta) \tag{3}$$

For t-channel,

$$\frac{\mathrm{d}\sigma}{\mathrm{d}\Omega}_t \sim (1-\cos^2\Theta)^{-2} \tag{4}$$

Forward-Backward Asymmetry is defined as

$$A_{FB} = \frac{N_+ - N_-}{N_+ + N_-} \tag{5}$$

where $N_{+,-}$ denotes number of events in forward or backward direction.

Near Z^0 resonance can be approximated by

$$\begin{aligned} A_{\mathrm{FB}}^f &\approx \frac{-3}{2} \frac{a_e a_f Q_f \,\mathrm{Re}(\chi)}{(v_e^2 + a_e^2)(v_f^2 + a_f^2)} \\ &= \frac{-3}{2} \frac{a_e a_f Q_f}{(v_e^2 + a_e^2)(v_f^2 + a_f^2)} \frac{s(s - M_Z^2)}{(s - M_Z^2)^2 + (s\Gamma_Z / M_Z)^2} \end{aligned} \tag{6}$$

3. Pre-lab tasks

Using equation (1), one finds

$$\Gamma_e = \Gamma_\mu = \Gamma_\tau = 83.40\,\mathrm{MeV} \tag{7}$$

The decay widths to leptons of three generations are the same because of lepton universality and neglecting the masses. With the same equation, decay width to quarks in total is

$$\begin{aligned} \Gamma_u = \Gamma_c &= 285.34\,\mathrm{MeV} \\ \Gamma_d = \Gamma_s = \Gamma_b &= 367.79\,\mathrm{MeV} \end{aligned}$$

It is significantly larger, since there are more quarks in SM and quarks carry more degrees of freedom (color) than leptons. Decays to neutrinos are invisible for detector in LEP, but still they have the width of

$$\Gamma_\nu = 165.84\,\mathrm{MeV} \tag{8}$$

Hadronic part

$$\Gamma_{\mathrm{h}} = \sum_{\forall q \neq t} \Gamma_q = 1674.06\,\mathrm{MeV} \tag{9}$$

Charged decay

$$\Gamma_{\mathrm{charged}} = 3\Gamma_e = 250.17\,\mathrm{MeV} \tag{10}$$

Invisible decay

$$\Gamma_{\mathrm{inv}} = 3\Gamma_\nu = 497.52\,\mathrm{MeV} \tag{11}$$

In total (except unknown decays)

$$\Gamma_{\mathrm{total}} = 3\Gamma_e + \Gamma_h + 3\Gamma_\nu = 2421.75\,\mathrm{MeV} \tag{12}$$

Assume that there is another generation of light fermions, the total width of Z^0 would be

$$\Gamma'_{\mathrm{total}} = \Gamma_{\mathrm{total}} + \Gamma_e + \Gamma_\nu + \Gamma_u + \Gamma_d = 3324.11\,\mathrm{MeV} \tag{13}$$

It would be a change of 37% percent!

The differential cross section $\frac{\mathrm{d}\sigma}{\mathrm{d}\Omega}$ has different angular dependencies for s- and t-channels, see equations (3) and (4). Simply plotting without the proportional constant in front shows where

decay type	partial width/MeV	partial cross section/10^{-5}MeV^{-2}
hadronic	1674.06	10.79
charged	250.17	1.61
invisible	497.52	3.21
total	2421.75	15.61

Table 1: Decays widths and partial cross sections

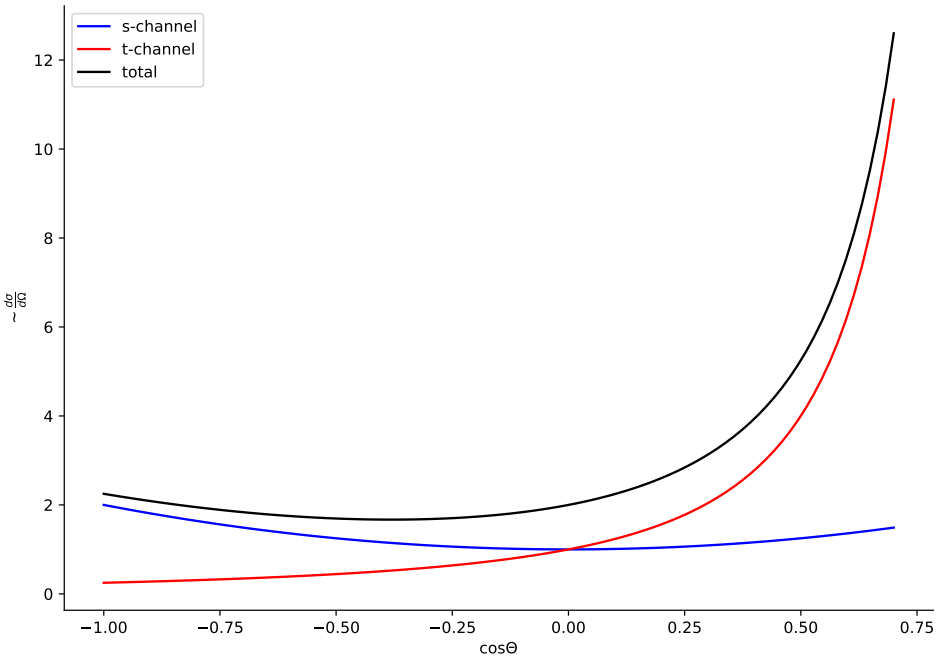

Figure 1: Angular dependencies of two channels.

s- or t-channels dominates the process, see figure. 1. At small angles, t-channel dominates, whereas at large angles, s-channel dominates.

Energy[GeV] /$\sin^2(\theta_W)$	0.21	0.23	0.25
89.225	−0.0379	−0.0420	−0.0451
91.225	−0.0386	−0.0428	−0.0459
93.225	−0.0394	−0.0436	−0.0468

4. Event display

5. Statistical Analysis

5.1. Mode selection

With large datasets, previous "event display" method will no longer be efficient and accurate. Thus data analysis tools are necessary. Here `root` is used and three macros to apply cuts are already implemented. As before we have four sets of Monte Carlo simulated data in order to find the optimal cuts, then there are a couple of real data samples.

First of all, there are a couple of general cuts. The collider energy of LEP is $\sim 200\,\text{GeV}$. Thus the scalar sum of momenta should be maximally around this value. Events with even larger momenta are caused by various unphysical processes. Secondly, the data here is written such as when there are multiple outgoing positive particles, `cos_thet` $= 1000$. For ee and $\mu\mu$ process, it should not be possible, since no hadronisation can occur and initial/final state radiation for these two only involve photons. So for these two event selections, cut `cos_thet` $<= 1.0$ is applied, see figure 2. After the cut(s), there are 56613 ee events, 89646 $\mu\mu$ events, 79099 $\tau\tau$ events, and 98100 qq events.

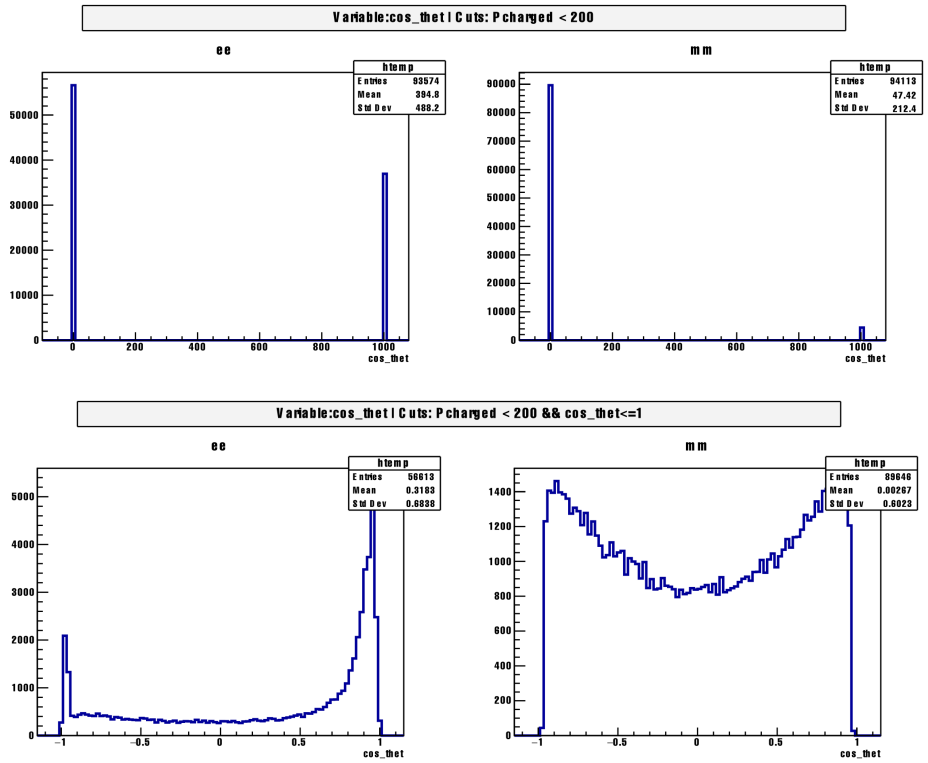

Figure 2: Distribution of `cos_thet` before and after `cos_thet` cut.

In event display part, we had success using cut `Ncharged` > 7 for qq processes. We conclude that this is no longer sufficient, since there are quite many $\tau\tau$ contamination, see figure 3. While roughly 5% percent of qq events are lost, $\tau\tau$ events are barely present and ee, $\mu\mu$ are completely cut. So the 5% percent are considered as acceptable "casualties". After the cut for qq, no ee or $\mu\mu$ are left, 78 $\tau\tau$ survives and 92688 qq events remain.

Follow the same receipt as in event display part, we try to separate ee events from other leptonic channels. Cut in number of charged track remains the same: `Ncharged` < 4 or (≤ 3). Same as before `E_ecal` of ee events have peak at around 80 GeV. `E_ecal` cut is changed to `E_ecal` > 60, since there is virtually no events even at `E_ecal` $= 60$, see figure 4. `E_hcal` cut is similar to before, just relaxed a little bit (to `E_hcal < 2`), since some of events have higher `E_hcal` as previous cut, see figure 5. In the end, we end up with 51679 ee events, 0 $\mu\mu$, 910 $\tau\tau$ events, and 1 qq event.

For $\mu\mu$ selection, cut in `Ncharged` is the same as ee: `Ncharged < 4`. We have already seen in figure 4 that `E_ecal` of $\mu\mu$ has a peak around 0, so the `E_ecal` cut for ee gets inverted as cut for $\mu\mu$: `E_ecal` < 60. Then remaining $\tau\tau$ events can be excluded with the help of `Pcharged`, see figure 6. ee and qq events are basically cut away, only unwanted events are $\tau\tau$. `Pcharged` distributions of $\mu\mu$ and $\tau\tau$ are separated quite nicely, although some $\mu\mu$ events have `Pcharged` ≈ 0. A cut at `Pcharged` > 70 will remove most of $\tau\tau$ events while preserve most of $\mu\mu$ events. After combinations of these cuts, 144 ee events, 83228 $\mu\mu$ events, 480 $\tau\tau$ events and zero qq event survive.

$\tau\tau$ can be picked out using the same cuts for $\mu\mu$ expect `Pcharged` cut gets inverted. Since there is a small peak at `Pcharged` $= 0$ in ee and $\mu\mu$ events, see figure 6, a lower bound in `Pcharged` should be set as well. Thus for $\mu\mu$: $1 <$ `Pcharged` < 60. E_ecal cut should be adjusted a bit. In figure 4, there are still quite substantial amount of $\tau\tau$ event between $60 <$ `E_ecal` < 70. Thus we have for $\tau\tau$: `E_ecal` < 70. Cut in `Ncharged` is relaxed to < 5 for better efficiency. After all these cuts, we have 243 ee events, 1446 $\mu\mu$ events, 66990 $\tau\tau$ events, and 38 qq events.

All the cuts are summarizes in table 2

mode	`cos_thet`	`Pcharged`	`Ncharged`	`E_ecal`	`E_hcal`
ee	≤ 1	< 200	< 4	> 60	< 2
$\mu\mu$	≤ 1	$> 70, < 200$	< 4	< 60	
$\tau\tau$		$> 1, < 60$	< 5	< 70	
qq		< 200	> 10		

Table 2: All cuts applied to select decay modes

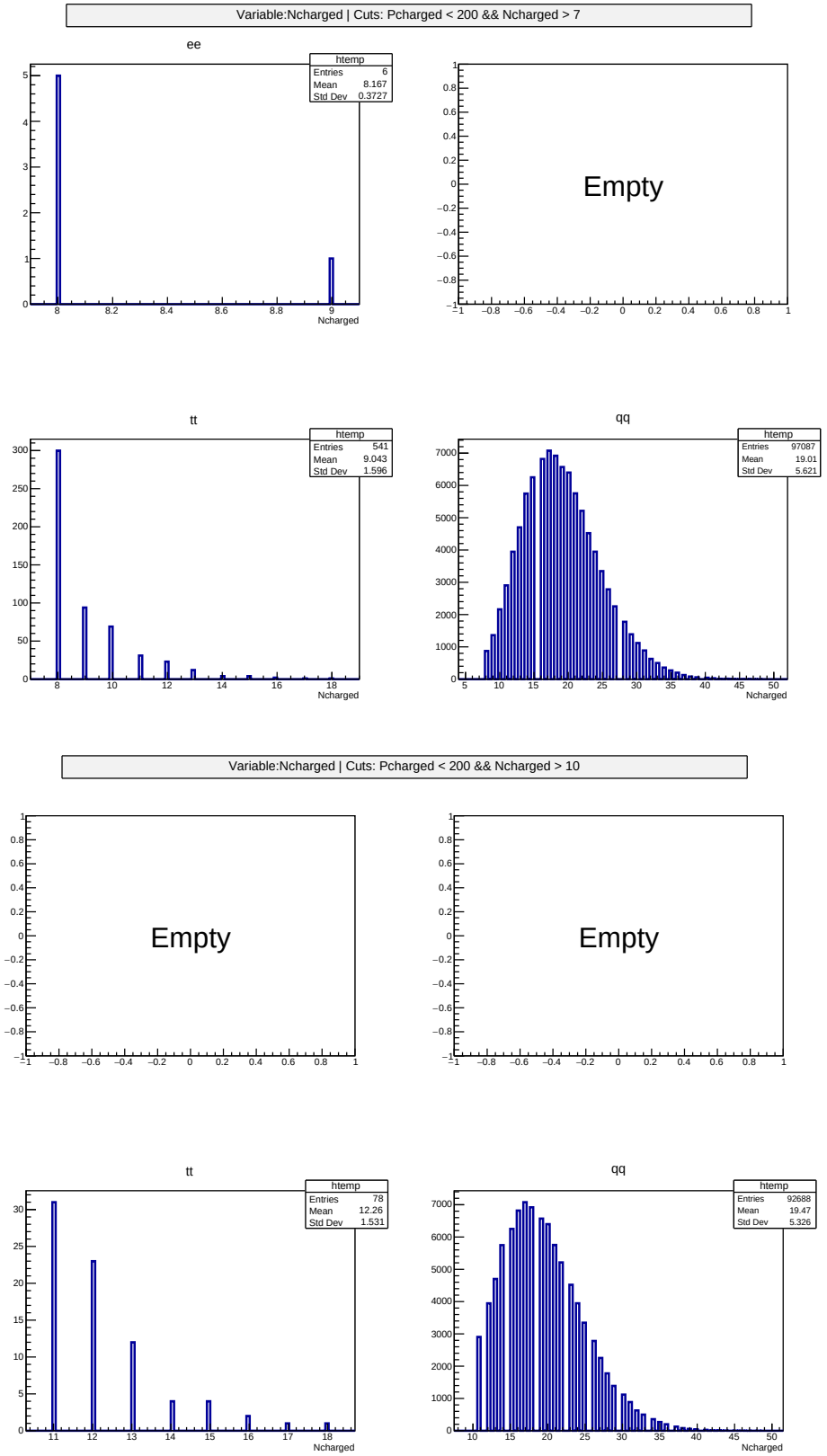

Figure 3: Number of charged tracks (`Ncharge`) before and after the refined cut for qq events.

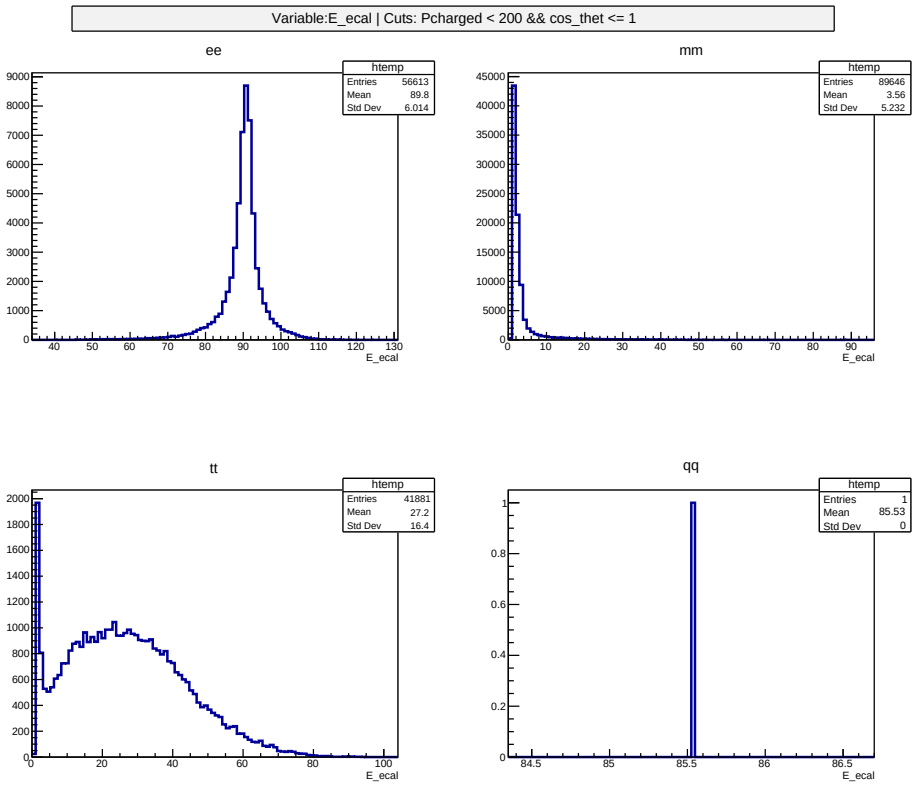

Figure 4: `E_ecal` distribution before `E_ecal` cut for ee.

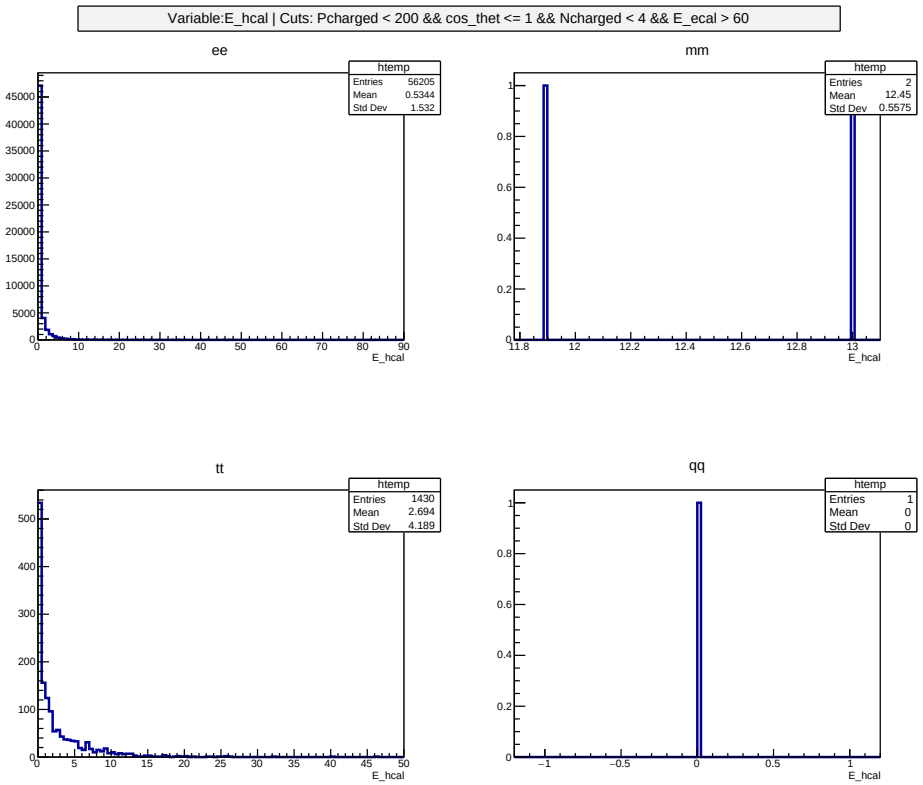

Figure 5: `E_hcal` distribution after `E_ecal` but before `E_hcal` cut for ee.

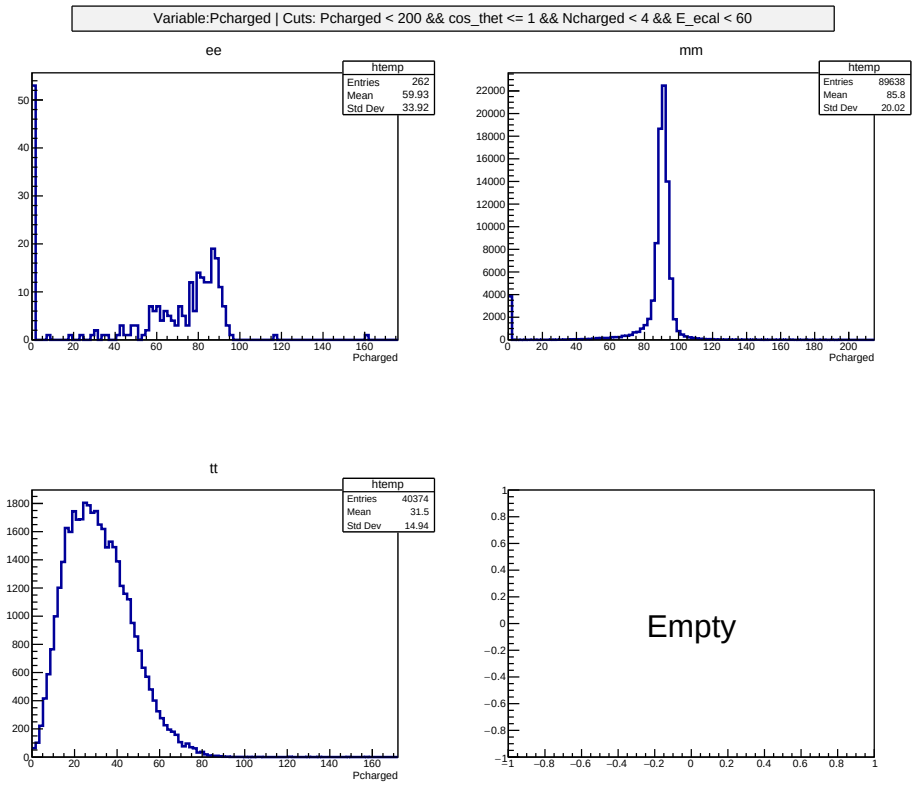

Figure 6: `Pcharged` distribution after `E_ecal` cut for $\mu\mu$.

5.2. Channel selection

Since processes with e^+e^- as final states include also t-channel elastic scattering between electron and positron and they are irrelevant processes in our discussion, we want to somehow get rid of these contributions. From figure 1 in pre-lab tasks, we know that s-channel dominates at small $\cos\Theta$ and s-channel contributions should look like symmetric around $\cos\Theta = 0$. Naturally, first thing comes in our minds is to cut $\cos\Theta$ from somewhere between 0 and 1 to $-\infty$, so that it looks symmetric. Figure 7 is done with $\cos\Theta < 0.5$. There is a quite significant peak around $\cos\Theta = -1$, which we don't really expect. Physical origin of this peak is unknown to us, but anyway this should be cut away. In the end, we have the cut $-0.9 < \cos\Theta < 0.5$. This cut along with the previous ee cuts will be the new ee cuts used onwards.

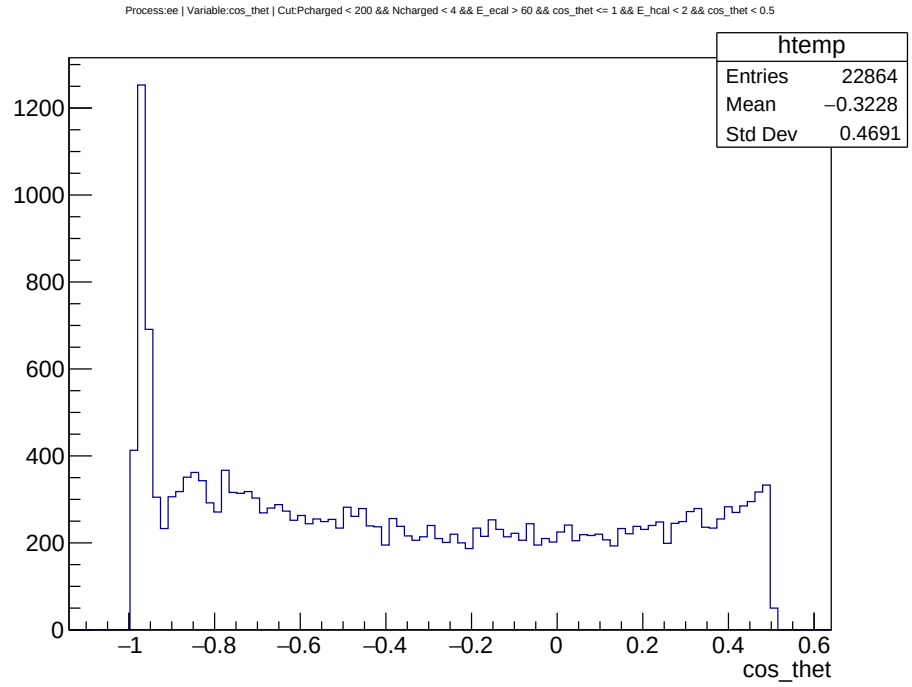

Figure 7: $\cos\Theta$ distribution of ee events after previously determined ee cuts and $\cos\Theta < 0.5$.

5.3. Forward-backward asymmetry

Numbers of events in forward ($0 < \cos\theta < 1$) and backward ($-1 < \cos\theta < 0$) are measured using `data1.root` and MC data with $\mu\mu$ as final states. In the actual analysis, only the real data are used. Upon inspection of definition 5, it is clear that correction for cut efficiency is unnecessary here, since $N_{+,-}$ share the same cuts.

After application of equation 5 at all available CMS energy, correction terms should be added to the measured asymmetry. As we understand it, applying these corrections will remove radiation corrections in measured data, so that we can directly compare experimental values with tree-level theoretical values.

Figure 8 shows the forward-backward asymmetry at various CMS energies. Errors are calculated as usual $\sigma_N \approx \sqrt{N}$.

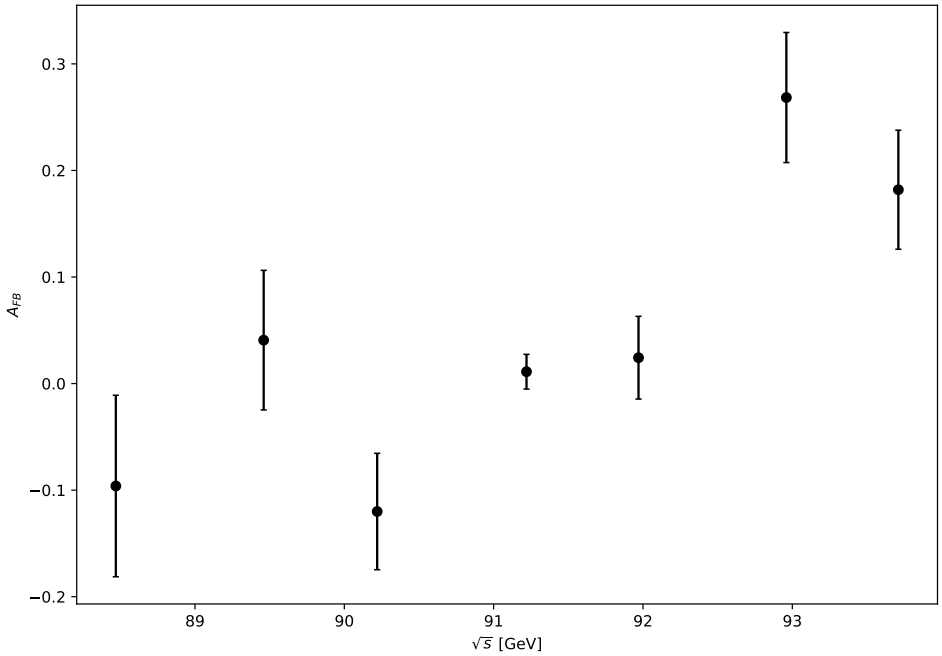

Figure 8: Forward-backward asymmetry after applying corrections.

If one says that the fourth data point (with $\sqrt{s} = 91.22\,\text{GeV}$) lies *exactly* at the peak of resonance, this A_{FB} can be used to determined the Weinberg angle

$$\sin^2\theta_W = \frac{1 - \sqrt{A_{\text{FB}}^{\mu,\text{peak}}/3}}{4}$$
$$\sigma_{\sin^2\theta_W} = \frac{1}{8\sqrt{3}}\frac{\sigma_A}{\sqrt{A}}$$

Then we have

$$\sin^2\theta_W = 0.2347 \pm 0.0112 \tag{14}$$

In principle one can calculate the Weinberg angle at every CMS energy using equation 6. But then according to QFT, value of Weinberg angle also changes, since it depends on the coupling g and g'. Thus we just settle with this value as our final result.

5.4. Cut efficiency

Cut efficiency can be defined as

$$\epsilon_{ij} = \frac{N_i}{N_j} \tag{15}$$

where a cut i is applied to a process j. In previous sections, there are multiple cuts and MC simulation data. By applying all the cuts to all the data, a 4×4 efficiency matrix can be

obtained.

$$\epsilon = \begin{pmatrix} N_{ee,\text{cuts}}/N_{ee} & N_{ee,\text{cuts}}/N_{\mu\mu} & N_{ee,\text{cuts}}/N_{\tau\tau} & N_{ee,\text{cuts}}/N_{qq} \\ N_{\mu\mu,\text{cuts}}/N_{ee} & N_{\mu\mu,\text{cuts}}/N_{\mu\mu} & N_{\mu\mu,\text{cuts}}/N_{\tau\tau} & N_{\mu\mu,\text{cuts}}/N_{qq} \\ N_{\tau\tau,\text{cuts}}/N_{ee} & N_{\tau\tau,\text{cuts}}/N_{\mu\mu} & N_{\tau\tau,\text{cuts}}/N_{\tau\tau} & N_{\tau\tau,\text{cuts}}/N_{qq} \\ N_{qq,\text{cuts}}/N_{ee} & N_{qq,\text{cuts}}/N_{\mu\mu} & N_{qq,\text{cuts}}/N_{\tau\tau} & N_{qq,\text{cuts}}/N_{qq} \end{pmatrix} \tag{16}$$

$$= \begin{pmatrix} 0.9667 \pm 0.0096 & 0.0000 \pm 0.0000 & 0.0082 \pm 0.0003 & 0.0000 \pm 0.0000 \\ 0.0070 \pm 0.0006 & 0.9284 \pm 0.0045 & 0.0061 \pm 0.0003 & 0.0000 \pm 0.0000 \\ 0.0153 \pm 0.0009 & 0.0317 \pm 0.0006 & 0.8881 \pm 0.0046 & 0.0004 \pm 0.0001 \\ 0.0000 \pm 0.0000 & 0.0000 \pm 0.0000 & 0.0010 \pm 0.0001 & 0.9448 \pm 0.0043 \end{pmatrix}$$

Raw data can be found in appenfix A.2. Note that the total number of events considered here is the number *after* `Pcharged` and `cos_thet` (including s-channel selection) cuts. After all, cuts efficiencies we discuss here are only the efficiencies of cuts like ee cuts and so on.

Error is estimated using Poisson statistic and usual error propagation formula.

$$\sigma_{\epsilon_{ij}} = \sqrt{\left(\frac{1}{N_j}\sigma_{N_i}\right)^2 + \left(\frac{N_i}{N_j^2}\sigma_{N_j}\right)^2} = \sqrt{\frac{N_i}{N_j^2} + \frac{N_i^2}{N_j^3}}$$

Actually the $\epsilon_{i,ee}$ efficiencies are problematic, because in `cos_thet` cuts, one part of s-channel gets lost. Main purpose of efficiency matrix is to obtain true number of events from measured number of events. If we continue to use $\epsilon_{i,ee}$ without further corrections, the true number of events are of $-0.9 <$ `cos_thet` < 0.5, resulting lower counts.

The correction involves adjustment of denominator or $\epsilon_{i,ee}$, since in selecting N_{ee} the s-channel cuts are applied. For this, the function $(1+\cos^2\Theta)$ is integrated in $-0.9 < \cos\Theta < 0.5$ and in $-1 < \cos\Theta < 1$.

$$\text{corr. factor} = \frac{\int_{-1}^{1} \mathrm{d}x\,(1+x^2)}{\int_{-0.9}^{0.5} \mathrm{d}x\,(1+x^2)} \approx 1.583 \tag{17}$$

This number is then multiplied to all the denominator of first column in equation 16. Now the corrected efficiency matrix is

$$\epsilon = \begin{pmatrix} 0.6107 \pm 0.0061 & 0.0000 \pm 0.0000 & 0.0082 \pm 0.0003 & 0.0000 \pm 0.0000 \\ 0.0044 \pm 0.0004 & 0.9284 \pm 0.0045 & 0.0061 \pm 0.0003 & 0.0000 \pm 0.0000 \\ 0.0097 \pm 0.0006 & 0.0317 \pm 0.0006 & 0.8881 \pm 0.0046 & 0.0004 \pm 0.0001 \\ 0.0000 \pm 0.0000 & 0.0000 \pm 0.0000 & 0.0010 \pm 0.0001 & 0.9448 \pm 0.0043 \end{pmatrix} \tag{18}$$

5.5. Partial cross sections

From last section, cut efficiency matrix is obtained. It describes how true numbers of events T_i translate into measured numbers of events M_i, i.e.

$$\mathbf{M} = \epsilon\mathbf{T} \tag{19}$$

In this compact matrix notation, $\mathbf{M}$ and $\mathbf{T}$ are vectors containing the numbers of events in a decay mode.

With real data in `data1.root`, we have the measured numbers using the cuts defined earlier. To find out true numbers, one needs to find inverse matrix ϵ^{-1}.

$$\mathbf{T} = \epsilon^{-1}\mathbf{M} \tag{20}$$

We are aware that we can propagate errors in ϵ and $\mathbf{M}$ to obtain an accurate error estimation of $\mathbf{T}$. According to [2],

$$\mathrm{Cov}(\epsilon^{-1}_{\alpha\beta}, \epsilon^{-1}_{ab}) = ([\epsilon^{-1}]_{\alpha i}[\epsilon^{-1}]_{ai})[\sigma_\epsilon]^2_{ij}([\epsilon^{-1}]_{j\beta}[\epsilon^{-1}]_{jb}) \tag{21}$$

and the correlation matrix of $\mathbf{T}$ is

$$\mathrm{Cov}(T_i, T_j) = M_\alpha M_\beta \mathrm{Cov}(\epsilon^{-1}_{i\alpha}, \epsilon^{-1}_{j\beta}) + \epsilon^{-1}_{ik}\epsilon^{-1}_{jl}\mathrm{Cov}(M_k, M_l) \tag{22}$$

where $\mathrm{Cov}(M_k, M_l)$ is generally diagonal. For simplicity, we neglect first term in equation 22. This is well justified, since errors in $\mathbf{T}$ are generally a couple of magnitudes larger than errors in ϵ. In the end, we want the diagonal entries of $\mathrm{Cov}(T_i, T_j)$, thus

$$\sigma^2_{T_i} = \epsilon^{-1}_{ik}\epsilon^{-1}_{ik}\sigma^2_{M_k} \tag{23}$$

After correction for efficiency, number of events needs to be subtracted by integrated luminosity $\int \mathrm{d}t\, \mathcal{L}$ to obtain partial differential cross section.

6. Conclusion and outlook

A. Appendix

A.1. Table for Question 5.6

Event	Ctrk(N)	Ctrk(Sump)	Ecal(SumE)	Hcal(SumE)	Comment
1	2	50.9	82.6	0.0	
2	2	91.0	90.0	0.0	
3	3	82.5	92.3	0.0	
4	2	80.9	86.8	0.0	
5	2	38.1	89.5	0.0	
6	2	83.8	87.5	0.0	
7	2	87.4	93.2	0.0	
8	2	69.3	90.7	0.0	
9	2	86.1	89.4	0.5	
10	2	90.3	90.6	0.0	
11	2	92.1	88.5	0.4	
12	3	81.7	91.6	0.0	
13	2	89.6	92.5	0.0	
14	2	61.1	89.2	0.0	
15	3	88.4	89.1	0.0	
16	2	90.9	90.5	0.3	
17	2	64.6	88.8	0.0	
18	2	95.6	96.2	0.0	
19	2	93.0	90.8	0.0	
20	2	94.1	89.2	0.0	

Table 3: caption

A.2. Raw data for cut efficiency

cuts	N_{ee}	$N_{\mu\mu}$	$N_{\tau\tau}$	N_{qq}
None	93 802	94 381	79 214	98 563
`Pcharge` and `cos_thet`	20 499	89 646	79 099	98 100
ee	19 817	0	651	0
$\tau\tau$	144	83 228	480	0
$\mu\mu$	314	2841	70 250	39
qq	0	0	78	92 688

Table 4: Raw data for efficiency matrix. N_i here refers to number of events in process i after some specificied cuts. Naturally ee and etc. cuts contain the `Pcharged` and `cos_thet` cuts, in particular for ee `cos_thet` cuts are so chosen that (almost) only s-channel events are selected.

A.3. Raw data for partial differential cross section

$\sqrt{s}$[GeV] or cuts	none	ee	$\mu\mu$	$\tau\tau$	qq
88.47	6194	125	136	157	3359
90.46	7861	198	233	207	5036
90.22	9779	223	329	249	7157
91.22	114 394	2313	3761	3247	87 844
91.97	18 931	346	664	538	14 571
92.96	8599	139	257	248	6303
93.71	10 125	191	318	281	7029

Table 5: Number of events with corresponding cms energy and cuts.

References

[1] Unknown. *E213 Analysis of Z0 Decay*. 2019.

[2] M Lefebvre et al. "Propagation of Errors for Matrix Inversion". In: *Nucl. Instrum. Methods Phys. Res., A* 451.hep-ex/9909031 (2000), pp. 520–528. URL: `https://cds.cern.ch/record/400631`.